Original

Kalanda, N.; Yarmolich, M.; Gurskii, A.; Petrov, A.; Zhaludkevich, A.; Ignatenko, O.; Serdechnova, M.:

Oxygen nonstoichiometry and magnetic properties of doped manganites La0.7Sr0.3Mn0.95Fe0.05O3-δ.

In: Modern Electronic Materials. Vol. 7 (2021) 4, 141 - 149.

First published online by Pensoft: 30.12.2021

https://dx.doi.org/10.3897/j.moem.7.4.80758

MOEM

Modern Electronic Materials 2021; 7(4): 141–149
DOI 10.3897/j.moem.7.4.80758

Research Article

Oxygen nonstoichiometry and magnetic properties of doped manganites $La_{0.7}Sr_{0.3}Mn_{0.95}Fe_{0.05}O_{3-\delta}$

Nikolay A. Kalanda[1], Marta V. Yarmolich[1], Alexander L. Gurskii[2], Alexander V. Petrov[1], Aliaksandr L. Zhaludkevich[1], Oleg V. Ignatenko[1], Maria Serdechnova[3]

1 Scientific-Practical Materials Research Centre of the NAS of Belarus, 19 P. Brovka Str., Minsk 220072, Belarus

2 Belarusian State University of Informatics and Radioelectronics, 6 P. Brovka Str., Minsk 220013, Belarus

3 Helmholtz-Zentrum Hereon, Max-Planck-Straße 1, Geesthacht 21502, Germany

Corresponding author: Nikolay A. Kalanda (kalanda@physics.by)

Received 1 December 2021 ♦ **Accepted** 14 December 2021 ♦ **Published** 30 December 2021

Citation: Kalanda NA, Yarmolich MV, Gurskii AL, Petrov AV, Zhaludkevich AL, Ignatenko OV, Serdechnova M (2021) Oxygen nonstoichiometry and magnetic properties of doped manganites $La_{0.7}Sr_{0.3}Mn_{0.95}Fe_{0.05}O_{3-\delta}$. *Modern Electronic Materials* 7(4): 141–149. https://doi.org/10.3897/j moem.7.4.80758

Abstract

In this work, solid solutions of $La_{0.7}Sr_{0.3}Mn_{0.95}Fe_{0.05}O_{3-\delta}$ with different oxygen content were obtained by the solid-phase reactions technique. Based on the investigation of the dynamics of changes in the oxygen index $(3 - \delta)$ during heating of the samples, the formation of a stressed state in their grains as a result of annealing was established. This results in a decrease in the mobility of oxygen vacancies during the reduction of cations according to the $Mn^{4+} + e^- \rightarrow Mn^{3+}$ scheme and explains the decrease of released oxygen amount with an increase of δ as well as the heating rate of the samples. When studying the magnetic properties of the obtained samples, it was found that the temperature dependence of the magnetization obeys the Curie–Weiss law and as the oxygen defficiency increases, the Curie temperature for solid solutions decreases. It was found that the particles are in a frozen ferromagnetic state when measured in the low-temperature region of the $M(T)$ dependence in "zero-field mode" at $T < T_B$. The presence of ferromagnetism at $T > T_B$ leads to a magnetically ordered state, in which the resulting magnetic moment of the magnetic particle is influenced by thermal fluctuations. When considering the temperature values of the magnetization of lanthanum-strontium manganite samples, it was found that with an increase of temperature in the low-temperature region, magnetic ordering is disturbed due to the excitation of magnons with a quadratic dependence of the energy from the wave vector, the number of which increases in proportion to $T^{3/2}$. This results in a decrease in the manganite magnetization. The observed temperature dependence of the magnetization measured in the "field-cooling mode" was approximated taking into account the quadratic and non-quadratic dispersion laws of the magnon spectrum.

Keywords

doped manganites, oxygen nonstoichiometry, temperature dependence of magnetization, Curie temperature, Bloch constant, exchange interaction constant.

1. Introduction

Noticeable interest to doped manganites with general formula $La_xR_{1-x}MnO_{3-\delta}$ (where R is a rare earth element), as strongly correlated electronic systems, can be associated with the existence of competing electron-electron and electron-phonon interactions that contribute to formation of spatially separated ferromagnetic and antiferromagnetic regions [1–3]. The presence of orbital and charge ordering in such systems stimulates the appear-

ance of giant magnetoresistance, spin-polarized electric transport, and other practically important characteristics [4–9]. The most promising is the partially substituted lanthanum strontium manganite of the composition $La_{0.7}Sr_{0.3}Mn_{0.95}Fe_{0.05}O_{3-\delta}$, which is characterized by the maximum values of the magnetoresistive effect near the "ferro-paramagnetic" phase transition. With the partial substitution of Fe^{3+} cations to Mn^{3+}, competition is observed between the exchange interactions Fe^{3+}—Mn^{3+} (antiferromagnetic) and Mn^{3+}—Mn^{4+} (ferromagnetic), which is caused by double Zener exchange [10–13]. Such manganite has a unique relationship between electrical, magnetic and other properties. It is also characterized by oxygen nonstoichiometry and is promising for use as a cathode material [10–14].

In early studies [10–15] it was found that for $La_{0.7}Sr_{0.3}Mn_{0.95}Fe_{0.05}O_{3-\delta}$, there is a transition from a paramagnet to a ferromagnet at the Curie temperature T_C. At the same temperature range, the high-temperature "insulating" phase undergoes a transition to the "metallic" phase. To explain this behavior, Zener double exchange mechanism was introduced [10–15], which later turned out to be insufficient to explain the large increase in resistance in the high-temperature region and its sharp drop in the low-temperature region. It was suggested that other effects resulting from Jahn–Teller distortions of the Mn^{3+} ion (electron-phonon, electron-magnon, and electron-polaron scattering of free charge carriers) may contribute to the electrical resistance [10–15]. In this case, the transformation of Mn^{3+}—O—Mn^{4+} chain, in which a double exchange is realized, can also occur due to the replacement of trivalent manganese by trivalent iron [5, 10–15]. It is also interesting because Fe doping is possible to a large extent, and Fe cation has uncompensated spins [10–15]. With the partial substitution of Fe for Mn in $La_{0.7}Sr_{0.3}Mn_{1-x}Fe_xO_3$, a significant change in the density of states near the Fermi level and a decrease in T_C values are observed due to both the antiferromagnetic interaction between Fe^{3+} and Mn^{3+} ions and the effect of cationic disordering in the Mn site.

It is known that in $La_{0.7}Sr_{0.3}MnO_{3-\delta}$ – manganites the value of δ cannot be higher than 3, since at $\delta > 3$ the perovskite structure is unstable and attempts to obtain compositions with $\delta > 3$ lead to the appearance of vacancies in the manganese and rare-earth sublattices [16–26]. In this case, the physico-chemical properties of manganite with the composition $La_{0.6}Sr_{0.4}MnO_{3-\delta}$ largely depend on the oxygen nonstoichiometry, which affects the oxidation state of manganese (Mn^{4+} and Mn^{3+} with electronic configurations $t_{2g}^3e_g^1$ ($S = 2$) and $t_{2g}^3e_g^0$ ($S = 3/2$), respectively) and electronic exchange between Mn^{3+} and Mn^{4+} [16–26]. Crystal lattice distortions caused by defectiveness in the anion sublattice affect the bonds and the spatial arrangement of the Mn^{4+}—O—Mn^{3+} chains, changing the magnitude of exchange interactions that depend both on the overlap of electron orbitals and on the bond angle between them. In this case, with a change in the oxygen deficiency δ and Mn cations, the sign of the exchange constant $J_{n,n+p}$, which is included in the Heisenberg-type Hamiltonian, changes:

$$H_{cx} = \frac{1}{2}\sum_{n,p} J_{n,n+p} S_n S_{n+p},$$

where the spins of S_n and S_{n+p} cations n and $n + p$ are located at the nearest neighboring nodes. In this case, the value of the constant $J_{n,n+p}$ is determined by the superexchange interaction through the p_σ and p_π states of the O^{2-} anions [16–26].

To purposefully optimize the production of $La_{0.7}Sr_{0.3}Mn_{0.95}Fe_{0.05}O_{3-\delta}$ with specified magnetic properties, it is important to establish the relationship between the macroscopic and microscopic parameters of the material, at which the saturation magnetization, and the general course of the temperature dependence are determined by microscopic parameters: the Bloch constant (B_T) and exchange interaction (A). The main point in calculating the above parameters, which are the key characteristics that determine the applied properties of a magnet, is the assumption that the easy magnetization axes in $La_{0.7}Sr_{0.3}Mn_{0.95}Fe_{0.05}O_{3-\delta}$ – grains are oriented randomly. In addition, in the ensemble of polydisperse particles there is a scatter in size, which affects the uncontrollability and irreproducibility of their properties. Despite the fact that the magnetic properties of $La_{0.7}Sr_{0.3}Mn_{0.95}Fe_{0.05}O_{3-\delta}$ have been widely studied by various authors, nevertheless, to date, there is no complete clarity in their understanding. Thus, it has not yet been established how the oxygen nonstoichiometry of the $La_{0.7}Sr_{0.3}Mn_{0.95}Fe_{0.05}O_{3-\delta}$ – samples affects their magnetic characteristics. In this regard, the study of oxygen desorption and magnetic properties will make it possible to control the conditions for optimal saturation and uniform oxygen distribution in the anionic sublattice and obtain reproducible magnetic characteristics necessary to increase the service life of sensor devices based on them.

2. Experimental

When preparing $La_{0.7}Sr_{0.3}Mn_{0.95}Fe_{0.05}O_{3-\delta}$ – solid solutions, La_2O_3, Mn_2O_3, Fe_2O_3 metal oxides and strontium carbonate $SrCO_3$ of the "high-purity" grade have been used. Heat treatment of the samples was carried out in resistive thermal units, the temperature in which was maintained using a high-precision temperature controller RIF-101 and controlled by a Pt–Pt/Rh (10%) thermocouple with an accuracy of ±0.5 K. To remove crystallization moisture, the initial chemical compounds were kept in a thermal installation for 10 h at a temperature of 1120 K. A stoichiometric mixture of the starting metal oxides and strontium carbonate was stirred in the ethyl alcohol and dried at 370 K until the alcohol was completely removed. Preliminary annealing was carried out in air at 1170 K for 18 h. Secondary grinding was used to increase the homogenization of the charge. Then

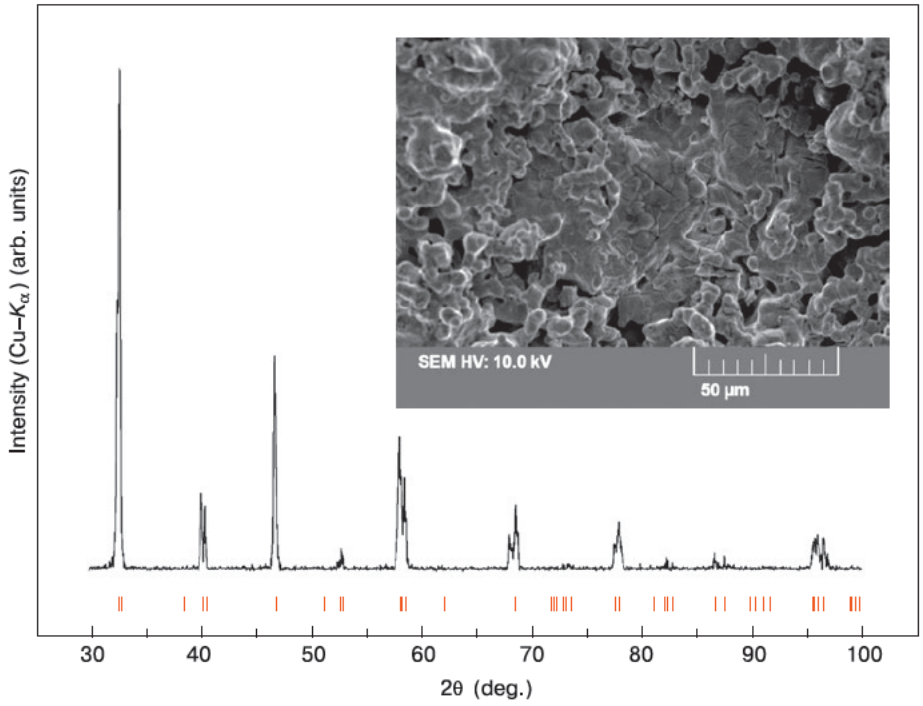

Figure 1. XRD pattern of the $La_{0.7}Sr_{0.3}Mn_{0.95}Fe_{0.05}O_{2.98}$ sample with a rhombohedral structure $(R\bar{3}c)$.

the powder was pressed into tablets with a diameter of 10 mm and a thickness of 4–5 mm under a force of 1500 kg. The synthesis of $La_{0.7}Sr_{0.3}Mn_{0.95}Fe_{0.05}O_{3-\delta}$ – samples was carried out in air at 1770 K with holding for 3 h, followed by cooling in the switched-off thermal installation mode.

The phase composition and crystal lattice parameters were determined using the ICSD – PDF2 database (Release 2000) and the PowderCell software [27], FullProf [28] by the Rietveld method based on X-ray diffraction data. Diffraction patterns were recorded at room temperature at a rate of 60°/h in the range of angles θ = 10–90° using the DRON-3 setup in CuK_α-radiation. According to the data of X-ray phase analysis, the single-phase composition of the $La_{0.7}Sr_{0.3}Mn_{0.95}Fe_{0.05}O_{2.98}$ – samples was established (Fig. 1).

The investigation of the nature of oxygen desorption by lanthanum-strontium manganite, as well as the preparation of samples with the required oxygen content was carried out by means of the thermogravimetry **(TGA)** at a heating rate of 2.5 K/min in a flowing gas stream of 1% H_2 + Ar using a SETARAM SetSys 16/18 system. A sign of reaching equilibrium was the coincidence of the sample mass at the same temperatures during the increase and decrease of the temperature.

Scanning electron microscopy **(SEM)** investigations have been carried out by means of the Vega 3 Tescan set up, suitable for operation in both high –vacuum and low –vacuum modes. The set up is equipped with LaB6 filament with best resolution of 2 nm at 30 kV in high-vacuum mode and 2.5 nm at 30 kV in low-vacuum mode. Magnification from 4× to 1 000 000× was selected.

The magnetic characteristics of the samples were studied on a Cryogenic Limited universal set up. The temperature dependences of magnetization were measured in two modes, with preliminary cooling from 500 to 4.2 K in a magnetic field (**FC** – field cooling) or without it (**ZFC** – zero-field cooling), followed by heating to 500 K in a magnetic field of 0.86 T

3. Results and discussion

In the work, the dynamics of changes in the oxygen index $(3-\delta)$ was investigated during heating of the samples at a rate of 2.5 deg/min to a temperature of 1270 K, followed by holding until thermodynamic equilibrium with the gas phase was established (Fig. 2).

Upon heating at a rate of υ = 2.5 deg/min, the first minimum of the time derivative of the oxygen index $T_1\{\min(d(3-\delta)/dt)_{2.5deg/min}\}$ = 739 K was observed with a smooth transition to the second weak one, which stood out as an independent extremum at $T_2\{\min(d(3-\delta)/dt)_{2.5deg/min}\}$ = 889 K. With an increase in the heating rate from 2.5 deg/min to 9 deg/min, the temperature of the first minimum shifts towards higher temperatures and corresponds to $T_1\{\min(d(3-\delta)/dt)_{9deg/min}\}$ = 882 K. In this case, the presence of the second minimum was not detected, but only a slight bend has been observed at $T_2\{\min(d(3-\delta)/dt)_{9deg/min}\}$ = 987 K.

When considering the amount of desorbed oxygen during heating from 300 K to 1270 K and holding until the thermodynamic equilibrium of the sample with the gas phase was established, it was found that the

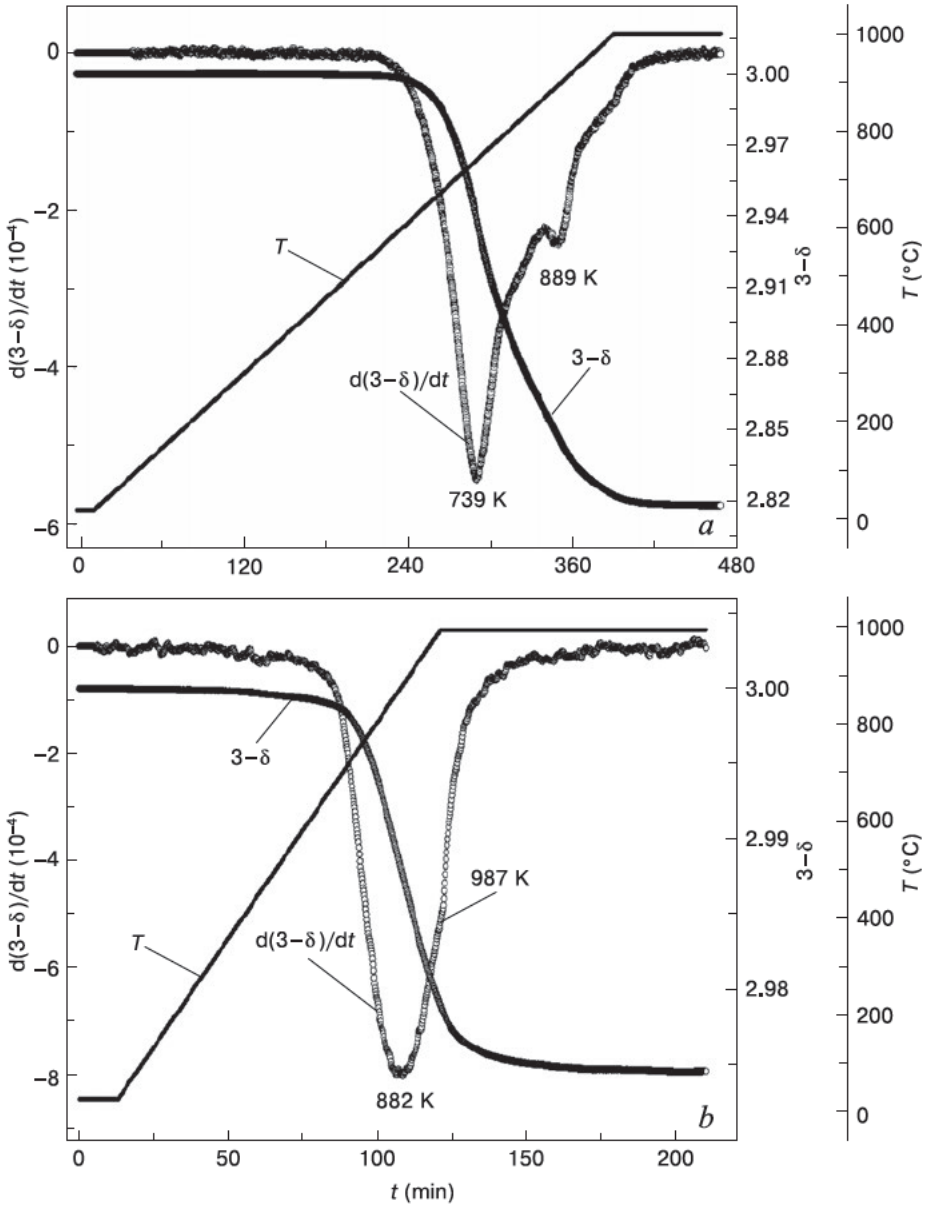

Figure 2. Change in the value of the oxygen index $(3-\delta)$ and its derivative $d(3-\delta)/dt$ during thermal action on the sample $La_{0.7}Sr_{0.3}Mn_{0.95}Fe_{0.05}O_{3-\delta}$ at heating rates of 2.5 deg/min (*a*) and 9 deg/min (*b*) in a gas flow of 1% H_2/Ar.

values $(3-\delta)_{300\to1270}$ increased with a decrease of the heating rate to υ = 2.5 deg/min, while at υ = 9 deg/min the rate of oxygen evolution decreased. This dependence $(3-\delta)_{300\to1270} = f(\upsilon)$ is most likely due to the appearance of additional kinetic difficulties in the diffusion of oxygen in $La_{0.7}Sr_{0.3}Mn_{0.95}Fe_{0.05}O_{3-\delta}$.

To substantiate the effect of the concentration of anionic vacancies on the oxygen mobility in iron-doped lanthanum-strontium manganite, the features of defect formation in it can be considered. Anionic vacancies (V) are formed in the crystal lattice of $La_{0.7}Sr_{0.3}Mn_{0.95}Fe_{0.05}O_{3-\delta}$ when the oxygen index $(3-\delta)$ is less than three, with a simultaneous charge redistribution between the Mn^{3+} and Mn^{4+} cations. Taking into account the observance of electroneutrality during the reduction of lanthanum-strontium manganite cations, the quasi-chemical reaction of defect formation can be written in the following form Eq. (1):

$$La^{3+}_{0.7}Sr^{2+}_{0.3}Mn^{3+}_{0.65}Fe^{3+}_{0.05}Mn^{4+}_{0.3}O^{2-}_{3} \leftrightarrow La^{3+}_{0.7}Sr^{2+}_{0.3}Mn^{3+}_{0.65+2\delta}Fe^{3+}_{0.05}Mn^{4+}_{0.3-2\delta}O^{2-}_{2}\left(V_O^{\bullet\bullet}\right)_{\delta}O^{2-}_{1-\delta} + \delta O_2\uparrow. \quad (1)$$

It can be seen from Eq. (1) that with the increase of δ the concentration $[Mn^{4+}] = 0.3 - 2\delta$ decreases, and $[Mn^{3+}] = 0.65 + 2\delta$ increases, leading to an increase in exchange interactions responsible for antiferromagnetic properties.

Let us consider various forms of oxygen arrangement in the $La_{0.7}Sr_{0.3}Mn_{0.95}Fe_{0.05}O_{3-\delta}$ compound. The first and most reactive form is oxygen adsorbed by the grain surface, for desorption of which the samples were preliminarily annealed at 1170 K in an argon flow for 2 h. The remaining three forms: 1 – lattice oxygen, bound with trivalent and tetravalent manganese (moreover, Mn^{4+} cations cause two different forms of oxygen); 2 – excess superstoichiometric oxygen, partially compensating for the presence of Mn^{4+} cations and 3 – oxygen, restoring electroneutrality with a decrease in charge due to the introduction of Sr^{2+}. The oxygen bound to the Fe^{3+} cation was not considered in frames of the current investigation because of its low concentration. Based on the above, it can be assumed that $T_1\,(d(3-\delta)/dt)_{2\ 5deg/min}$ is due to the release of superstoichiometric oxygen and a decrease in the $[Mn^{4+}]$ concentration. With an increase in temperature, a significantly lower min $T_2\,(d(3-\delta)/dt)_{2\ 5deg/min}$ is observed, at which the bonds of anions with an octahedron are broken, in the center of which $Mn^{4+}(6)$ is located. This is apparently due to the fact that the force of electrostatic repulsion between the anions is higher than in octahedra with $Mn^{3+}(6)$ due to the difference in cationic radii ($r(Mn^{3+}(6)) = 0.0645$ nm, $r(Mn^{4+}(6)) = 0.0530$ nm) [16–17]. The appearance of $V_O^{\bullet\bullet}$ defects promotes the redistribution of the electron density, the reduction of the manganese cation Mn^{4+}, and the formation of Mn^{3+} in the pentahedral environment of the ligands with $r(Mn^{3+}(5)) = 0.0580$ nm. Upon reduction, the effective ionic radii of manganese cations, $r(Mn^{4+}(6)) = 0.0530$ nm, $r(Mn^{3+}(6)) = 0.0645$ nm and $r(Mn^{3+}(5)) = 0.0580$ nm differ significantly; therefore, an increase in the $[Mn^{3+}]$ radius in the octahedral and pentahedral environment of the ligands leads to an increase in the molar volume of manganite within the existence of a structure with the *RC* symmetry, as indicated by the by the XRD phase analysis data. Since an increase in the molar volume of manganite is observed during oxygen desorption, a stressed state in grains is formed in $La_{0.7}Sr_{0.3}Mn_{0.95}Fe_{0.05}O_{3-\delta}$, during annealing, which leads to a decrease in the mobility of $V_O^{\bullet\bullet}$ during the reduction of cations according to the $Mn^{4+} + e^- \rightarrow Mn^{3+}$ scheme. In this case, the rate of oxygen desorption is determined by its diffusion in the stressed regions of the grains. This explains the decrease in the amount of released oxygen with an increase in δ and the heating rate of $La_{0.7}Sr_{0.3}Mn_{0.95}Fe_{0.05}O_{3-\delta}$ samples (Fig. 2).

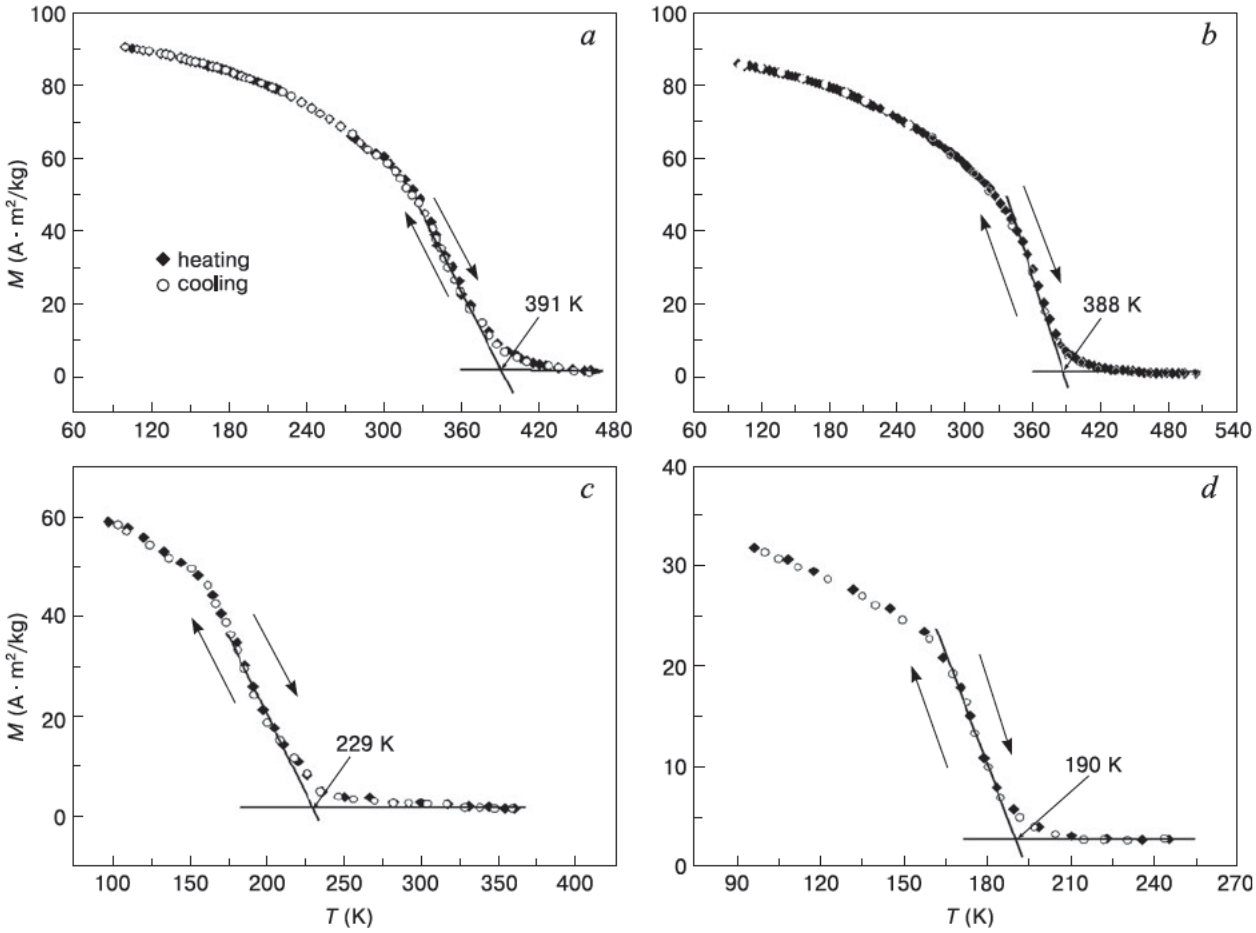

Figure 3. Temperature dependence of the magnetization of the compositions $La_{0.7}Sr_{0.3}Mn_{0.95}Fe_{0.05}O_{3-\delta}$: δ = 0.02 (*a*), δ = 0.08 (*b*), δ = 0.15 (*c*), δ = 0.18 (*d*), investigated in magnetic field 8.6 kOe.

Following the presented above, the effect of oxygen nonstoichiometry on the magnetic properties of manganite can be considered. Figure 3 shows the temperature dependence of the magnetization $M(T)$ of the $La_{0.7}Sr_{0.3}Mn_{0.95}Fe_{0.05}O_{3-\delta}$ system with different $3-\delta$ oxygen content in a magnetic field H = 8.6 kOe (Fig. 3).

It was found that the temperature dependence of the magnetization obeys the Curie–Weiss law and the values of the magnetization parameters are presented in Table 1.

It can be seen from Figs. 3 and 4, that at low temperatures the magnetization weakly depends on T. However, with temperature increase, a decrease begins on the $M(T)$ curves, which continues in a wide temperature range. Obviously, the concept of the Curie temperature T_C of samples in an insulating magnetically two-phase state, such as the studied compositions $La_{0.7}Sr_{0.3}Mn_{0.95}Fe_{0.05}O_{3-\delta}$, is rather arbitrary. It is also incorrect to determine T_C from the magnetization in weak magnetic fields, since this magnetization is mainly due to the demagnetizing factor. The demagnetizing factor of the ferromagnetic phase depends on its configuration, which changes with temperature. Therefore, as the Curie temperature, the temperature obtained by extrapolating the steepest part of the $M(T)$ curve, measured at the magnetic field strength H = 8.6 kOe, before its intersection with the temperature axis. T_C values are presented in the Table 1 for all studied samples. Table 1 shows that as the oxygen deficiency increases, the Curie temperature decreases. It was found that above T_C there is a "tail" of magnetization, while the difference in magnetization values at 300 and 5 K increases with decreasing oxygen index (Figs. 3 and 4). This is additional evidence of the magnetic inhomogeneity of the samples.

Table 1. Fitting coefficients and calculated magnetic characteristics of a magnet obtained by approximating the temperature dependence of magnetization by function (2)

δ	T_C (K)	M_{T0} (A·m²/kg)	B_T (K$^{-3/2}$)	C_T (K$^{-5/2}$)	A (J·m^{-1})	R^2
$La_{0.7}Sr_{0.3}Mn_{0.95}Fe_{0.05}O_{3-\delta}$						
0.02	391	92.28	$1.60\cdot10^{-5}$	$2.69\cdot10^{-5}$	$4.92\cdot10^{-12}$	0.9998
0.08	388	86.40	$3.09\cdot10^{-5}$	$6.76\cdot10^{-5}$	$3.10\cdot10^{-12}$	0.9992
0,15	229	66.10	$4.92\cdot10^{-5}$	$2.33\cdot10^{-5}$	$2.08\cdot10^{-12}$	0.9995
0,18	190	35.34	$8.92\cdot10^{-5}$	$1.97\cdot10^{-5}$	$1.14\cdot10^{-12}$	0.9995

Note: R^2 – coefficient of determination.

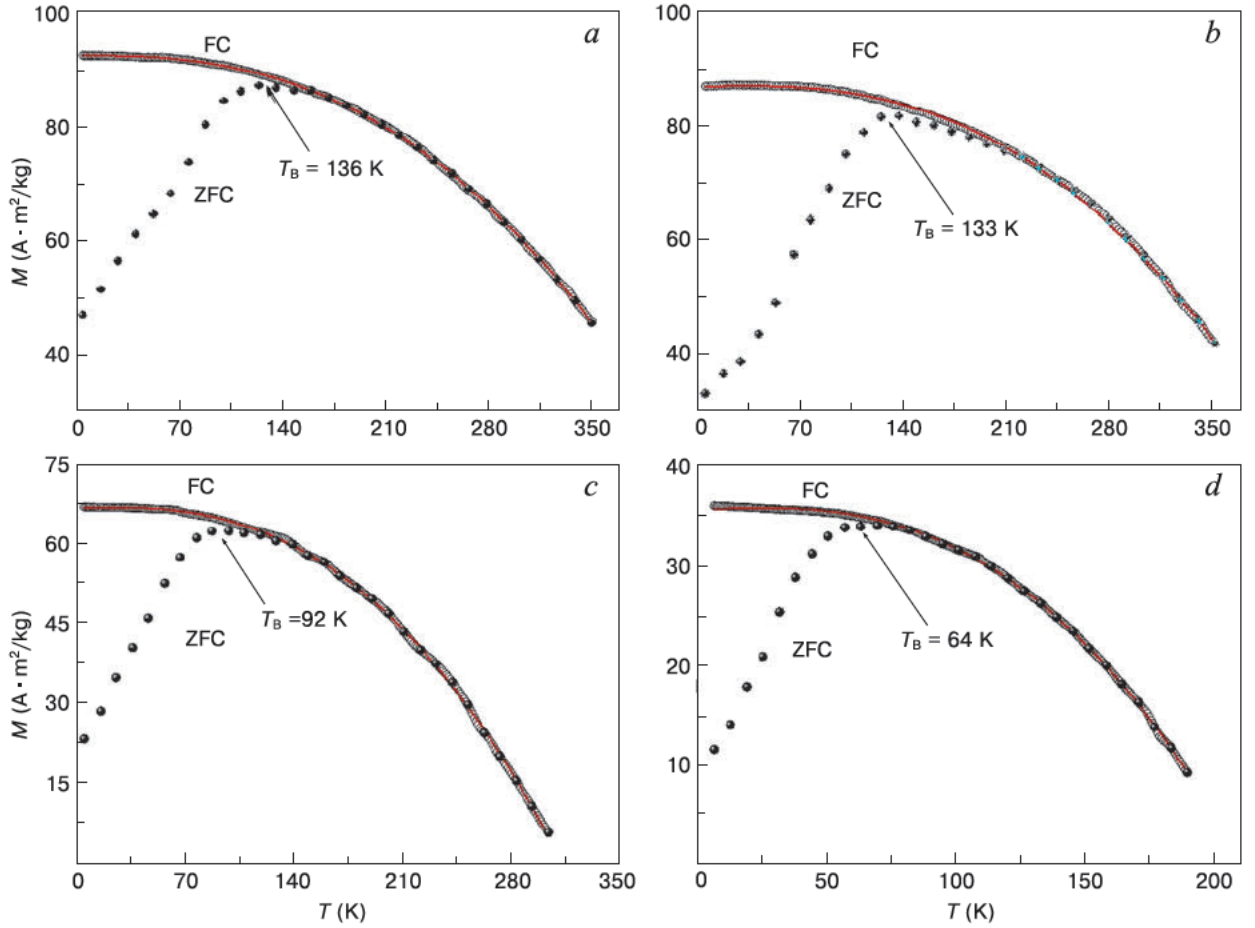

Figure 4. Temperature dependence of magnetization $M(T)$ for samples $La_{0.7}Sr_{0.3}Mn_{0.95}Fe_{0.05}O_{2.98}$ (*a*), $La_{0.7}Sr_{0.3}Mn_{0.95}Fe_{0.05}O_{2.92}$ (*b*), $La_{0.7}Sr_{0.3}Mn_{0.95}Fe_{0.05}O_{2.85}$ (*c*), $La_{0.7}Sr_{0.3}Mn_{0.95}Fe_{0.05}O_{2.82}$ (*d*), measured in a magnetic field H = 8.6 kOe in ZFC and FC modes, where black circles are experimental data, red line is approximation of experimental data by function (3).

Considering the low-temperature region of the $M(T)$ dependence, measured in the ZFC mode, it can be assumed that at $T < T_B$ (where T_B is the blocking temperature), the particles are in a frozen ferromagnetic state (Figs. 3 and 4). The presence of ferromagnetism at $T > T_B$ leads to a magnetically ordered state, in which the resulting magnetic moment of the magnetic particle is influenced by thermal fluctuations. It is shown that with an increase in oxygen deficiency, the T_B values decrease, which indicates an increase in the effect of magnetocrystalline anisotropy.

When considering the temperature values of $La_{0.7}Sr_{0.3}Mn_{0.95}Fe_{0.05}O_{3-\delta}$ sample magnetization, it was found that with an increase of temperature in the low-temperature region, magnetic ordering is disturbed due to the excitation of magnons with a quadratic dependence of the energy on the wave vector $E(k) \sim k^2$, the number of which increases in proportion to $T^{3/2}$, leading to a decrease in the magnetization of the manganite (Fig. 3). In this case, the temperature dependence of the magnetization, according to Bloch's law, should be presented in the following form Eq. (2):

$$M(T) = M_{T0}(1 - B_T T^{3/2}), \quad (2)$$

where M_{T0} is the average magnetization of ferrimagnetic particles at 4.2 K, B_T is an adjustable coefficient corresponding to the Bloch constant. It was found that the best approximation according to Bloch's law of the dependence $M(T)$ measured in an external magnetic field of 0.01 T was realized in the temperature range $4.2 < T < 100$ K. An increase of temperature promotes the excitation of magnons with large values of the wave vector **k**, characterized by non-square dispersion law and interacting with each other. In this regard, it is necessary to use corrections that take into account such effects. Dyson [29] showed that deviation from Bloch's law can be described in the model by including the term $C_T T^{5/2}$ according to equation Eq. (3):

$$M(T) = M_{T0}(1 - B_T T^{3/2} - C_T T^{5/2}), \quad (3)$$

where all the coefficients are positive and the third term is related to the non-square dispersion law of the magnon spectrum.

The exchange interaction constant A in the $La_{0.7}Sr_{0.3}Mn_{0.95}Fe_{0.05}O_{3-\delta}$ samples was determined from the Eq. (4):

$$A = \frac{k_B}{8\pi}\left(\frac{g\mu_B}{M_{T0}}\right)^{-\frac{1}{3}}\left(\frac{2{,}612}{B_T}\right)^{\frac{2}{3}}. \quad (4)$$

k_B is the Boltzmann constant, $g = 2.02$ is the Lande factor, μ_B is the Bohr magneton. The values obtained for magnets with different oxygen index contents are presented in Table 1. It was found that, according to Eq. (4), the exchange interaction constant A in the $La_{0.7}Sr_{0.3}Mn_{0.95}Fe_{0.05}O_{3-\delta}$ compound decreases with increasing oxygen nonstoichiometry.

4. Conclusion

In frames of the presented work an increase in the molar volume of manganite is observed during oxygen desorption. It results in a stressed state formation in grains of $La_{0.7}Sr_{0.3}Mn_{0.95}Fe_{0.05}O_{3-\delta}$ compound during annealing. This leads to a decrease in the mobility of oxygen vacancies during the reduction of cations according to the scheme $Mn^{4+} + e^- \rightarrow Mn^{3+}$. In this case, the rate of oxygen desorption is determined by its diffusion in the stressed regions of the grains. This explains the decrease in the amount of released oxygen with an increase of δ and the heating rate of the $La_{0.7}Sr_{0.3}Mn_{0.95}Fe_{0.05}O_{3-\delta}$ samples.

It was established that in the low-temperature region of the $M(T)$ dependence measured in the ZFC mode at $T < T_B$ the particles are in a frozen ferromagnetic state. The presence of ferromagnetism at $T > T_B$ leads to a magnetically ordered state, in which the resulting magnetic moment of the magnetic particle is influenced by thermal fluctuations. It was found that with an increase in oxygen deficiency, the T_B values decrease, which indicates an increase in the effect of magnetocrystalline anisotropy.

It was found that the observed temperature dependence of the magnetization measured in the FC mode was approximated taking into account the quadratic and non-quadratic dispersion laws of the magnon spectrum. The calculated values of the Bloch coefficients and the exchange interaction constant indicate their dependence on the composition of the magnetic.

It was demonstrated that the exchange interaction constant A in the $La_{0.7}Sr_{0.3}Mn_{0.95}Fe_{0.05}O_{3-\delta}$ compound decreases with increasing oxygen nonstoichiometry. In this work, the magnetic characteristics of manganites $La_{0.7}Sr_{0.3}Mn_{0.95}Fe_{0.05}O_{3-\delta}$, which are important for practical applications, are calculated, which can serve as a reference point in the development of new memory elements, magnetic field sensors with enhanced magnetic characteristics.

Acknowledgments

A support of the work in frames of the European Union project H2020-MSCA-RISE-2018-823942 – FUNCOAT and in frames of the project of the Belarusian Republican Foundation for Fundamental Research No. F21ISR-004 are gratefully acknowledged.

References

1. Goodenough J.B. Electronic and ionic transport properties and other physical aspects of perovskites. *Reports on Progress in Physics*, 2004; 67: 1915–1994. https://doi.org/10.1088/0034-4885/67/11/R01
2. Dunaevsky S.M. Magnetic phase diagrams of manganites in the area of their electronic doping (a Review). *Fizika Tverdogo Tela*, 2004; 46(2): 193–211. (In Russ.)
3. Balagurov A.M., Bushmeleva S.N., Pomjakushin V.Yu., Sheptyakov D.V., Amelichev V.A., Gorbenko O.Yu., Kaul A.R., Gan'shina E.A., Perkins N.B. Magnetic structure of $NaMnO_3$ consistently doped with Sr and Ru. *Phys. Rev. B*, 2004; 70: 014427. https://doi.org/10.1103/PhysRevB.70.014427
4. Kozlenko D.P., Glazkov V.P., Jirák Z., Savenko B.N. High pressure effects on the crystal and magnetic structure of $Pr_{1-x}Sr_xMnO_3$ manganites (x = 0.5–0.56). *J. Phys. Condensed Matter*, 2004; 16(13): 2381–2394. https://doi.org/10.1088/0953-8984/16/13/017
5. Nagaev E.L. Lanthanum manganites and other giant-magnetoresistance magnetic conductors. *Physics – Uspekhi*, 1996; 39(8): 781–806. https://doi.org/10.1070/ PU1996v039n08ABEH000161
6. Yanchevskii O.Z., V'yunov O.I., Belous A.G., Tovstolytkin A.I., Kravchik V.P. Synthesis and properties of $La_{0.7}Sr_{0.3}Mn_{1-x}Ti_xO_3$. *Fizika Tverdogo Tela*, 2006; 48(4): 667–673. (In Russ.)
7. McIntosh S., Vente J.F., Haije W.G., Blank D.H.A., Bouwmeester H.J.M. Structure and oxygen stoichiometry of $SrCo_{0.8}Fe_{0.2}O_{3-\delta}$ and $Ba_{0.5}Sr_{0.5}Co_{0.8}Fe_{0.2}O_{3-\delta}$. *Solid State Ionics*, 2006; 177(19–25): 1737–1742. https://doi.org/10.1016/j.ssi.2006.03.041
8. Maignan A., Martin C., Pelloquin D., Nguyen N., Raveau B. Structural and magnetic studies of ordered oxygen-deficient perovskites $LnBaCo_2O_{5+\delta}$, closely related to the "112" structure. *J. Solid State Chem.*, 1999; 142(2): 247–260. https://doi.org/10.1006/jssc.1998.7934
9. Yamazoe N., Furukawa S., Teraoka Y., Seiyama T. The effect of oxygen sorption on the crystal structure of $La_{1-x}Sr_xCoO_{3-\delta}$. *Chem. Lett.,* 1982; 11(12): 2019–2022. https://doi.org/10.1246/cl.1982.2019
10. Deshmukh A.V., Patil S.I., Bhagat S.M., Sagdeo P.R., Choudhary R.J., Phase D.M. Effect of iron doping on electrical, electronic and magnetic properties of $La_{0.7}Sr_{0.3}MnO_3$. *J. Phys. D Appl. Phys.*, 2009; 42(18): 185410. https://doi.org/10.1088/0022-3727/42/18/185410
11. Barik S.K., Mahendiran R. Ac magnetotransport in $La_{0.7}Sr_{0.3}Mn_{0.95}Fe_{0.05}O_3$ at low dc magnetic fields. *Solid State Communications*, 2011; 151(24): 1986–1989. https://doi.org/10.1016/j.ssc.2011.09.007
12. Ritter C., Ibarra M.R., Morellon L., Blasco J., Garcia J., De Teresa J.M. Structural and magnetic properties of double perovskites AA'$FeMoO_6$ (AA' = Ba_2, BaSr, Sr_2 and Ca_2). *J. Phys. Condensed Matter*, 2000; 12(38): 8295–8308. https://doi.org/10.1088/0953-8984/12/38/306
13. dos Santos–Gómez L., Leon-Reina L., Porras-Vazquez J.M., Losilla E.R., Marrero-Lopez D. Chemical stability and compatibility of double perovskite anode materials for SOFCs. *Solid State Ionics*, 2013; 239: 1–7. https://doi.org/10.1016/j.ssi.2013.03.005
14. Huang Q., Li Z.W., Li J., Ong, C.K. The magnetic, electrical transport and magnetoresistance properties of epitaxial $La_{0.7}Sr_{0.3}Mn_{1-x}Fe_xO_3$ (x = 0–0.20) thin films prepared by pulsed laser deposition. *J. Phys. Condensed Matter*, 2001; 13(18): 4033–4048. https://doi.org/10.1088/0953-8984/13/18/312
15. Kruidhof H., Bouwmeester H.J.M., v. Doorn R.H.E., Burggraaf A.J. Influence of order-disorder transitions on oxygen permeability through selected nonstoichiometric perovskite-type oxides. *Solid State Ionics*, 1993; 63–65: 816–822. https://doi.org/10.1016/0167-2738(93)90202-E
16. Kuo J.H., Anderson H.U., Sparlin D.M. Oxidation-reduction behavior of undoped and Sr-doped $LaMnO_3$: defect structure, electrical conductivity, and thermoelectric power. *J. Solid State Chem.*, 1990; 87(1): 55–63. https://doi.org/10.1016/0022-4596(90)90064-5
17. Ulyanov A.N., Mazur A.S., Yang D.C., Krivoruchko V.N., Danilenko I.A., Konstantinova T.E., Levchenko G.G. Local structural and magnetic inhomogeneities in nanosized $La_{0.7}Sr_{0.3}MnO_3$ manganites. *Nanosystems, Nanomaterials, Nanotechnologies*, 2011; 9(1): 107–114. (In Russ.)
18. Krivoruchko V.N., Marchenko M.A. Modeling of the hysteresis properties of the (LaSr)MnO_3 nanostructured samples. *Fizika Niskikh Temperatur*, 2008; 34(9): 947–955. (In Russ.)
19. Ziese M., Vrejoiu I., Setzer A., Lotnyk A., Hesse D. Coupled magnetic and structural transitions in $La_{0.7}Sr_{0.3}MnO_3$ films on $SrTiO_3$. *New J. Phys.*, 2008; 10: 063024. https://doi.org/10.1088/1367-2630/10/6/063024
20. Mizusaki J., Mori N., Takai H., Yonemura Y., Minamiue H., Tagawa H., Dokiya M., Inaba H., Naraya K., Sasamoto T., Hashimoto T. Oxygen nonstoichiometry and defect equilibrium in the perovskite-type oxides $La_{1-x}Sr_xMnO_{3+d}$. *Solid State Ionics*, 2000; 129(1–4): 163–177. https://doi.org/10.1016/S0167-2738(99)00323-9
21. Jimenes M., Martinez J.L., Herrero E., Alonso J., Prieto C., de Andres A., Vallet-Regi M., Gonzalez-Calbet J., Fernandez-Diaz M.T. Structural and magnetoresistance study of $La_xMn_yO_{3\pm z}$. *Phys. B Condensed Matter*, 1997; 234–236: 708–709. https://doi.org/10.1016/S0921-4526(96)01110-6
22. Aruna S.T., Muthuraman M., Patil K.C. Combustion synthesis and properties of strontium substituted lanthanum manganites $La_{1-x}Sr_xMnO_3$ ($0 \le x \le 0.3$). *J. Mater. Chem.*, 1997; 7(12): 2499–2503. https://doi.org/10.1039/A703901H
23. De Leon-Guevara A.M., Berthet P., Berthon J., Millot F., Revcolevschi A., Anane A., Dupas C., Le Dang K., Renard J.P., Veillet P. Influence of controlled oxygen vacancies on the magnetotransport and magnetostructural phenomena in $La_{0.85}Sr_{0.15}MnO_{3-\delta}$ single crystals. *Phys. Rev. B*, 1997; 56(10): 6031. https://doi.org/10.1103/PhysRevB.56.6031
24. Veverka P., Kaman O., Knížek K., Novák P., Maryško M., Jirák Z. Magnetic properties of rare-earth-doped $La_{0.7}Sr_{0.3}MnO_3$. *J. Phys. Condensed Matter*, 2016; 29(3): 035803. https://doi.org/10.1088/1361-648X/29/3/035803
25. Mizusaki J., Tagawa H., Naraya K., Sasamoto T. Nonstoichiometry and thermochemical stability of the perovskite-type $La_{1-x}Sr_xMnO_{3-\delta}$. *Solid State Ionics*, 1991; 49: 111–118. https://doi.org/10.1016/0167-2738(91)90076-N
26. Kuo J.H., Anderson H.U., Sparlin D.M. Oxidation-reduction behavior of undoped and Sr-doped $LaMnO_3$: defect structure, electrical conductivity, and thermoelectric power. *J. Solid State Chem.*, 1990; 87(1): 55–63. https://doi.org/10.1016/0022-4596(90)90064-5

27. Rodríguez-Carvajal J. Recent developments of the program FULL-PROF. Commission on powder diffraction (IUCr). *Newsletter*, 2001; 26: 12–19.
28. Kraus W. POWDER CELL – a program for the representation and manipulation of crystal structures and calculation of the resulting X-ray powder patterns. *J. Appl. Crystallography*, 1996; 29(3): 301–303. https://doi.org/10.1107/S0021889895014920
29. Dyson F.J. Thermodynamic behavior of an ideal ferromagnet. *Phys. Rev.*, 1956; 102(5): 1230–1244. https://doi.org/10.1103/PhysRev.102.1230